



AIAA 2001-1218

Detection of Micro-Leaks through  
Complex Geometries under Mechanical  
Load and at Cryogenic Temperature

H. K. Rivers and J. G. Sikora  
NASA Langley Research Center

S. N. Sankaran  
Analytical Services & Materials, Inc.  
Hampton, VA

**42nd AIAA/ASME/ASCE/AHS/ASC Structures,  
Structural Dynamics, and Materials Conf.  
& Exhibit**

16–19 April 2001  
Seattle Washington

## DETECTION OF MICRO-LEAKS THROUGH COMPLEX GEOMETRIES UNDER MECHANICAL LOAD AND AT CRYOGENIC TEMPERATURE<sup>1</sup>

H. Kevin Rivers\*  
Joseph G. Sikora\*  
Sankara N. Sankaran†

### Abstract

Polymer Matrix Composite (PMC) hydrogen tanks have been proposed as an enabling technology for reducing the weight of Single-Stage-to-Orbit reusable launch vehicles where structural mass has a large impact on vehicle performance. A key development issue of these lightweight structures is the leakage of hydrogen through the composite material. The rate of hydrogen leakage can be a function of the material used, method of fabrication used to manufacture the tank, mechanical load the tank must react, internal damage-state of the material, and the temperatures at which the tank must operate. A method for measuring leakage through a geometrically complex structure at cryogenic temperature and under mechanical load was developed, calibrated and used to measure hydrogen leakage through complex X-33 liquid-hydrogen tank structure sections.

### Introduction

Current research in reusable launch vehicles has focused on reducing the cost of delivering payloads to orbit [1]. An important aspect of reducing the cost of access to space is the reduction of launch vehicle weight. Liquid hydrogen (LH<sub>2</sub>) tanks can be the largest structural component of a launch vehicle and the design of lightweight hydrogen tanks is important to reducing the cost of space access. Polymer Matrix Composite (PMC) hydrogen tanks have been proposed as an enabling technology for reducing the weight of launch vehicles. A significant development issue of these composite structures is the leakage of hydrogen through the tank wall. Hydrogen is difficult to contain due to its small molecular size. Containment is critical due to its chemical reactivity. Concentrations of hydrogen in air above 4 percent by volume are flammable and hydrogen can detonate in air when concentrations reach 18.3 percent by volume [2]. Since the open cavities that may be filled with hydrogen are dependent on launch vehicle concepts, the acceptable hydrogen leak rate varies with each vehicle concept definition. For the National Aerospace Plane (NASP) and Single-Stage-to-Orbit (SSTO) vehicle definitions [3], acceptable minimum leak rates for the hydrogen tanks were based on the total level of leakage expected through fittings and valves and was calculated to be 10<sup>-4</sup> to 10<sup>-3</sup> SCC/sec.-in<sup>2</sup>.

The rate of hydrogen leakage can be a function of the material, the method of fabrication used, the internal damage-state of the material, mechanical load the tank must react, and operational temperature. Typical permeability tests are performed on small coupon specimens, without the complexities of mechanical or thermal loads, using helium or hydrogen as a test gas [4]. Although these tests are useful for screening materials and fabrication processes, they do not address the important issue of determining the in-situ rate of hydrogen leakage in built-up structural components exposed to temperature and mechanical loads.

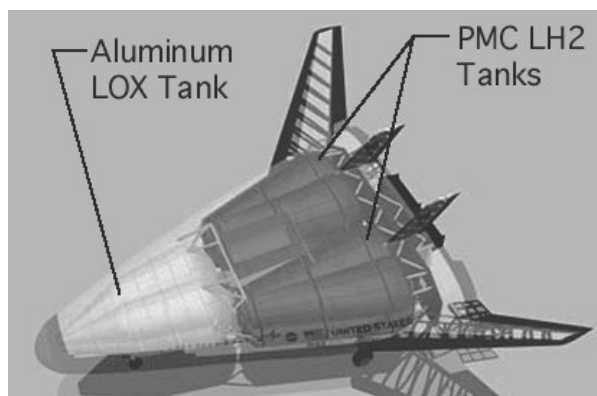


**Figure 1. The X-33 structural arrangement showing quad-lobed LH<sub>2</sub> tanks and dual-lobed liquid oxygen (LOX) tank.**

\* NASA Langley Research Center, Hampton, VA

† Analytical Services & Materials, Inc., Hampton, VA, currently with Lockheed-Martin Engineering and Sciences

<sup>1</sup> Copyright © 2001 by the American Institute of Aeronautics and Astronautics, Inc. No copyright is asserted in the United States under Title 17, U.S. Code. The U. S. Government has a royalty-free license to exercise all rights under the copyright claimed herein for Governmental purposes all other rights are reserved by the copyright owner.

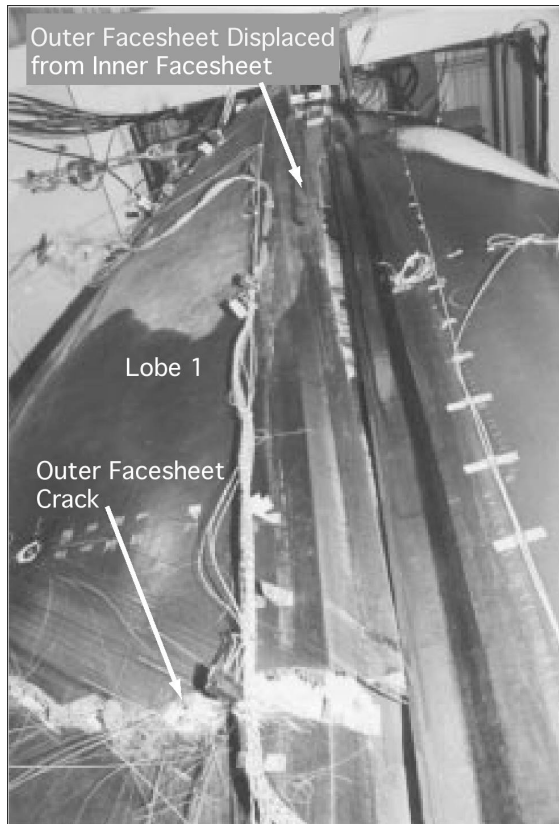


**Figure 2. A photograph of the failed X-33 LH<sub>2</sub> tank.**

Test methods and a test apparatus developed and validated for measuring the leakage of helium or hydrogen through complex, built-up structures, which can be mechanically loaded at cryogenic temperature, are presented herein. Descriptions of the test methods, test apparatus, calibration test results, and test specimens derived from the X-33 Program are reported. Results from helium and hydrogen leak tests for the X-33 specimens, performed at cryogenic temperatures, are also presented.

### **Background**

The Lockheed-Martin X-33 vehicle design incorporated two PMC LH<sub>2</sub> tanks. Shown in Figure 1, these tanks were quad-lobed tanks with honeycomb-core sandwich wall construction. Both face-sheets of the sandwich were Graphite-Epoxy (IM7/977-2) and the core material was Korex™† 3-pcf, unvented, aramid-phenolic honeycomb.

During preflight proof testing the first X-33 LH<sub>2</sub> tank failed when pressure increased in the core of

† The use of trade names does not imply endorsement by the National Aeronautics and Space Administration.

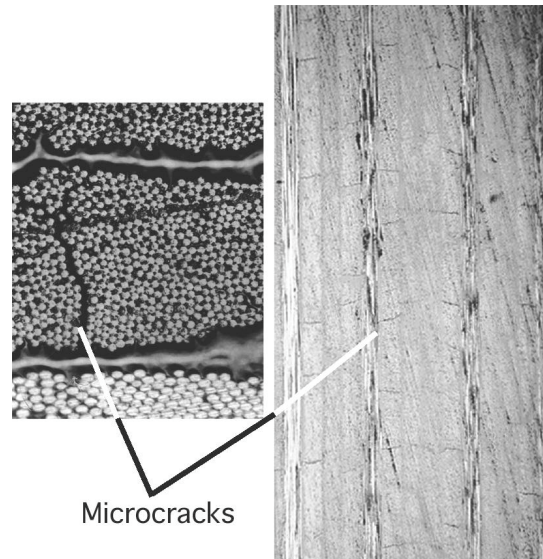


**Figure 3. Micrographs of sample microcracked composite materials.**

the sandwich tank wall causing the face-sheets to disbond and separate from the core material, as shown in Figure 2. An investigation team determined the most probable cause of the failure to be a combination of the following: microcracking of the inner face-sheet with subsequent gaseous hydrogen (GH<sub>2</sub>) infiltration, cryopumping of the exterior nitrogen purge gas, reduced bondline strength and toughness, and manufacturing flaws and defects [5].

Many factors contribute to the leakage of gases through materials. Porosity, manufacturing flaws, and internal damage each contribute to the permeability of a material. In PMC materials the greatest contributor to leakage is believed to be microcracks. Microcracks form leak paths that allow gases to pass through the material. Examples of typical microcracks in composite materials are shown in the micrographs in Figure 3.

As noted in the X-33 tank failure investigation report [5], most composite materials will microcrack at LH<sub>2</sub> temperature due to large transverse thermal residual stresses, large total stress levels, and low transverse matrix strength in the ply.

The following analysis, taken from Reference 5, demonstrates that when the residual stresses resulting from PMC laminate construction are included, the combination of residual thermal stress and applied mechanical stress can generate microcracks in a PMC material. Using Classical Lamination Theory, ply level residual stresses can be calculated. These stresses are high at cryogenic operating conditions and can contribute to the generation of microcracks.

$$\sigma_i^r = - Q_{ij} \epsilon_j (T - T_o) \quad (1)$$

where

$\sigma_i^r$  = components of the ply level residual thermal stress tensor

$Q_{ij}$  = components of the laminate stiffness matrix

$\epsilon_j$  = coefficients of thermal expansion of the matrix and fiber

$T$  = laminate temperature

$T_o$  = stress free temperature

(assumed to be 320°F).

Ply level mechanical stresses due to the tank internal pressure also contribute to the total stress.

$$\sigma_i^m = - Q_{ij} \epsilon_j \quad (2)$$

where

$\sigma_i^m$  = components of the ply level mechanical stress tensor

$\epsilon_j$  = applied strain tensor

For the X-33 LH<sub>2</sub> tank, ply transverse thermal residual stresses ( $\sigma_T^r$ ) are high enough to promote microcracking in the inner face-sheet. Shown below in equation 3, the ratio of  $\sigma_T^r$  to the ultimate stress in the 90° ply ( $\sigma_{ult}(ply,90^\circ)$ ) indicate that the stresses will exceed acceptable limits and cracking will occur.

$$(\sigma_T^r / \sigma_{ult}(ply,90^\circ)) \sim 0.8 - 1.8 \quad (3)$$

Coincidentally, the total ply transverse stresses ( $\sigma_T^r + \sigma_T^m = \sigma_T^{total}$ ) in the X-33 tank's outer face-sheet are also high enough to promote microcracking.

$$(\sigma_T^{total} / \sigma_{ult}(ply,90^\circ)) \sim 0.9 - 1.9 \quad (4)$$

It should also be noted that not only do the thermal and mechanical loads generate microcracking in PMC materials, but these loads can cause existing microcracks to open, increasing the rate of leakage through the material. For this reason, leakage should be studied while the material is at operational temperature and under mechanical load.

### Leak Testing

This study was motivated by the need to measure hydrogen leakage through actual X-33 tank structure while it was under mechanical load and at cryogenic temperature. The level of leakage must be considered when designing measurement systems. The anticipated leak levels were considered to be higher than typical permeation rates, which were less than 10<sup>-4</sup> SCC/sec./in<sup>2</sup>, but lower than leaks that were detectable with soap bubble techniques. For this reason, the measurement system was designed to measure micro-leaks, or leaks in the range of 10<sup>-4</sup>-10<sup>-2</sup> SCC/sec./in<sup>2</sup>.

### The Flexible Micro-Leak Detection System (FMLDS)

The FMLDS is shown schematically in Figure 4. The system consists of a flexible aluminized Mylar™ vacuum membrane, sealed to the test specimen with a vacuum seal material, and a micro-leak collection and measurement system. When tests are performed at

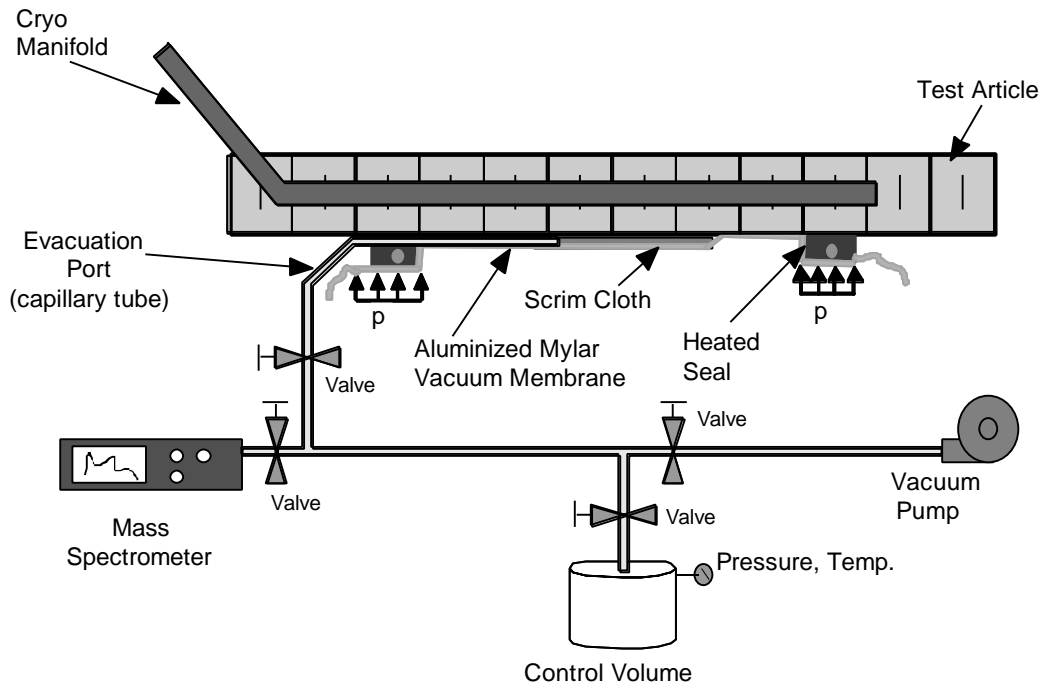
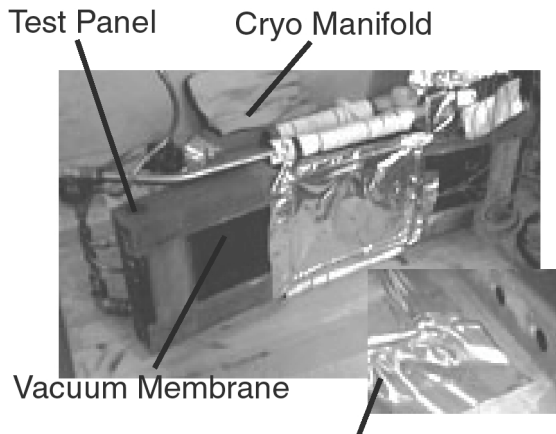


**Figure 4. The Flexible Micro-Leak Detection System (FMLDS).**



Close-up of Seal Corner

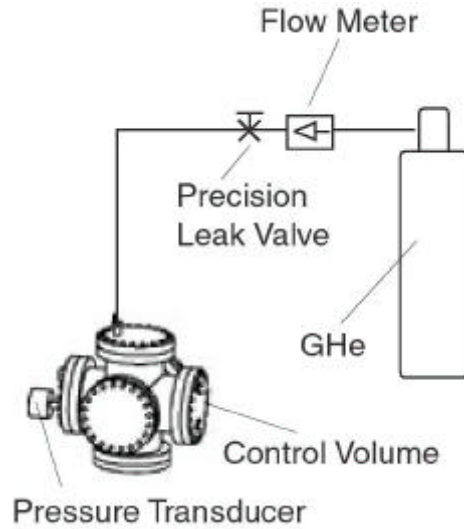
**Figure 5. Test panel with installed vacuum membrane and cryo manifold.**

cryogenic temperatures, compressed foam is used to maintain a slight positive pressure,  $p$ , on the seal. The seal must be kept above  $0^{\circ}\text{F}$  to maintain an acceptable vacuum seal. Heated ethylene glycol is circulated through a 0.125-in. copper tube embedded in the center of the seal. Gases that leak through the test specimen are captured in a space maintained by a scrim cloth under the vacuum membrane and are vented through a 0.0625-in. stainless-steel capillary tube to an evacuated control volume. The capillary tube is connected to the control volume through 0.25-in. stainless steel tubing. Leak measurements are made by monitoring the pressure rise and temperature change in the evacuated control volume and converting these changes to mass flow rates using the ideal gas law. A mass spectrometer used to determine the gas species leaking into the system verifies that the leak being measured is not from a source other than the test panel. In the event of very low leak rates (less than  $10^{-4}$  SCC/sec/in<sup>2</sup>) the mass spectrometer could be used to determine the permeation rate.

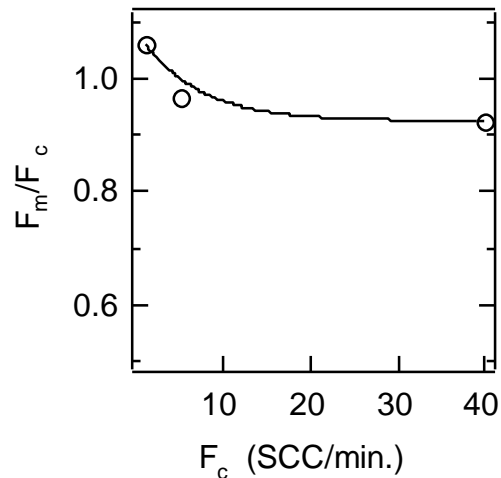
The photograph in Figure 5 shows the vacuum membrane sealed to an X-33 test specimen. Because the vacuum membrane and the sealing material are very flexible, they can be applied to complex geometric shapes and are easily field installed. Also, the test apparatus is portable and can be used nearly anywhere.

Calibration tests

The FMLDS was calibrated to determine its accuracy for a range of leakage flow rates with a known standard and the effects of cryogenic conditions on the entire FMLDS.



(a) Calibration setup.



(b) Calibration results.

**Figure 6. Flow calibration of the vacuum pressure measurement system.**

The first calibration test measured the accuracy of the flow rate measurements obtained from monitoring pressure rises in an evacuated control volume over time, as seen in the schematic of Figure 6(a). Gaseous helium (GHe) was flowed through a standard 50 SCC/min. flow meter, with an accuracy of 1% of the full scale, across a precision leak valve and into the evacuated control volume where pressure was measured. Measurements were made at 1, 5 and 40 SCC/min. by setting the precision leak valve and monitoring the level of flow registered on the flow meter. At each valve setting the pressure in the evacuated control volume was monitored over a two-minute period and the ideal gas law was used to compute a measured flow. The ratio of this measured flow rate,  $F_m$ , to the rate indicated by the flow meter,  $F_c$ ,

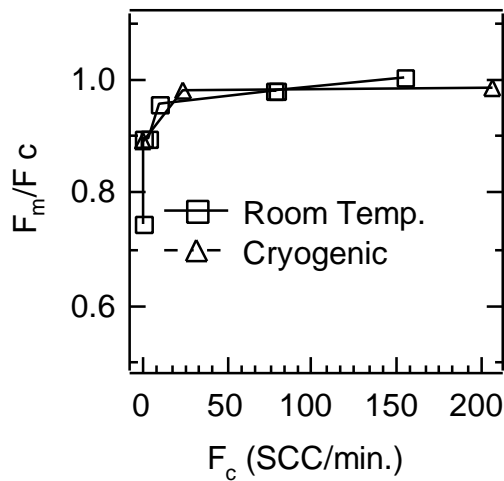
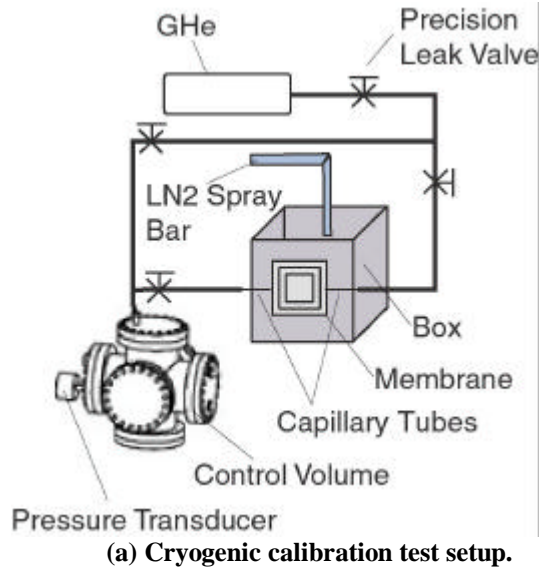


Figure 7. Calibration of the Flexible Micro-Leak Detection System.

is plotted in Figure 6(b). The error at the lowest level of flow (1 SCC/min.) was assumed to be contributed by the  $\pm 0.5$  SCC/min. accuracy of the flow meter. As shown in the figure, the measured flow rate is accurate to  $\pm 5$  percent at flow rates between 1 and 40 SCC/min.

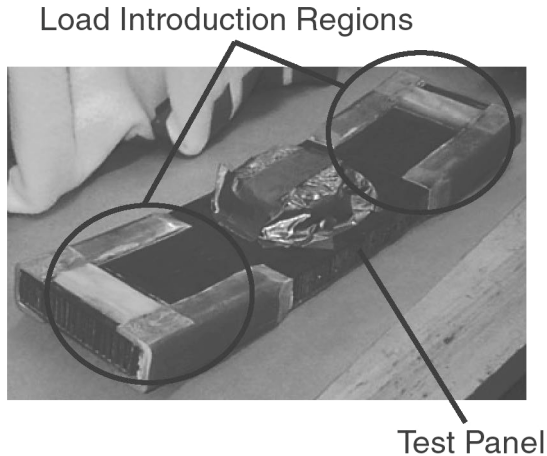
The second calibration test measured the overall accuracy of the FMLDS. This test was designed to measure the errors introduced by the flexible vacuum membrane, heated seal, capillary tubing used to collect leaking gases, and cryogenic temperatures. As seen in the schematic of Figure 7(a), the FMLDS was attached to the side of a 12-in. by 12-in. by 12-in., stainless steel container that was cooled with liquid nitrogen (LN<sub>2</sub>). Gaseous helium (GHe) was delivered through a precision leak valve to the FMLDS by 0.25-in. stainless steel tubing and a 0.0625-in., stainless-steel, capillary

tube. The gas was then removed from the vacuum membrane through a 0.0625-in. capillary tube passing through the seal material and connected through 0.25-in. stainless-steel tubing to the evacuated control volume where pressure and temperature were measured over time. The GHe could also be delivered directly to the control volume by using flow control valves to direct the flow through 0.25-in. stainless steel tubing which bypassed the FMLDS. Comparisons of the flow rate measured through this bypass line and through the FMLDS indicated the accuracy of the system at various settings of the precision leak valve (or at various leak levels).

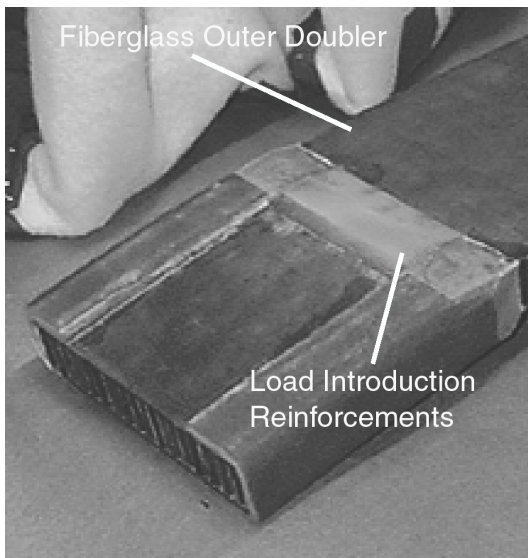
Flow calibration tests were first performed at room temperature, then the system was used to assess the functionality of the FMLDS seal at cryogenic temperature before cryogenic calibration tests were performed. It was observed that when the seal temperature fell below 0°F the seal failed and pressures in the control volume rose instantaneously to atmospheric pressure. For the cryogenic tests, the FMLDS seal was maintained at 10°F, near the lower limit of the recommended seal operating temperature of 0°F, by controlling the supply of liquid nitrogen to the stainless steel container through a spray bar. During these tests the flow of heated ethylene glycol through the seal-heating loop was maintained at its maximum level. Both the room temperature tests and tests at cryogenic temperature were performed with leak rates varying between zero and 200 SCC/min.

Table 1. Calibration test results.

Room Temperature Data		
F <sub>C</sub> SCC/min.	F <sub>M</sub> SCC/min.	Ratio (F <sub>M</sub> /F <sub>C</sub> )
0.113	0.084	0.75
0.662	0.594	0.90
2.578	2.31	0.90
9.001	8.637	0.96
78.1	76.58	0.98
77.93	76.5	0.98
154.0	154.5	1.00
Cryogenic Test Data		
F <sub>C</sub> SCC/min.	F <sub>M</sub> SCC/min.	Ratio (F <sub>M</sub> /F <sub>C</sub> )
0.311	0.277	0.89
24.346	23.861	0.98
206.38	203.346	0.98



**Figure 8. X-33 test article.**



**Figure 9. Specimen preparation details.**

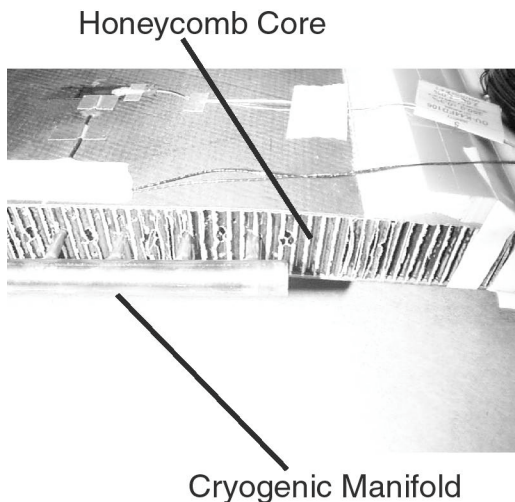


**Figure 10. Cryogenic manifold inserted into the honeycomb core.**

At each setting of the precision leak valve, the flow measured through the FMLDS ( $F_m$ ) and through the bypass line ( $F_c$ ) were collected then the ratio was plotted as a function of  $F_c$ , see Figure 7(b). Results from tests at room temperature and cryogenic temperature are also given in Table 1. At leak levels above 9 SCC/min., the error was approximately 2 percent. For leaks between 0.3 and 9 SCC/min., the error was about 10 percent. As leaks were reduced to 0.1 SCC/min., the error increased to 25 percent. It is believed that at these lower levels of leakage (with lower levels of pressure), the conductance through the 0.0625-in. capillary tube limited the flow and increased errors in the measurements, as seen in the data collected.

#### Test articles

Two test articles were evaluated for liquid helium (LHe) and LH<sub>2</sub> leakage in this study. Both specimens were cut from the scrapped lobe 4, LH<sub>2</sub> tank 1 of the X-33. This lobe was rejected due to manufacturing flaws. Both specimens were nominally 24-in. long and 7-in. wide. The specimens were curved with a radius of 65-in. the hoop direction and tapered slightly in the longitudinal direction.

The specimens were Graphite-Epoxy (IM7/977-2) sandwich construction consisting of an inner face-sheet of cross ply tape with a stacking sequence of [45/90<sub>3</sub>/-45/0<sub>1.5</sub>]<sub>s</sub> and an outer face-sheet with a stacking sequence of [65/0/-65/90<sub>0.5</sub>]<sub>s</sub>. Each laminate was robotically placed. The core material was Korex,<sup>TM</sup> 3/16-in. cell, 3-pcf, unvented, aramid-phenolic honeycomb.

In these tests, an in-plane tensile load was introduced to the inner face-sheet by loading the specimen in 4 point bending (4-pt. bending). Four-point bending was used to introduce load because the curvature in the specimen prevented using a conventional universal tension test setup. Because the core shear strength was very low, fiberglass reinforcements were added in the load introduction region (see Figure 8). Since the outer face-sheet was thinner, a layer of fiberglass material was added to it to prevent its failure. Both of these reinforcements can be seen in the photograph shown in Figure 9. The specimen's temperature was maintained at cryogenic temperature and the source for leak gas was provided by introducing cryogenic fluids into the core of the sandwich through a stainless steel manifold, see Figure 10. Ten 0.25-in. holes were machined in the core in the center 12 in. of the panel at 0.5 in. spacing to receive the manifold. Under 4-pt. bending the core shear was negligible in this area. Holes, 0.0625-in. in diameter,

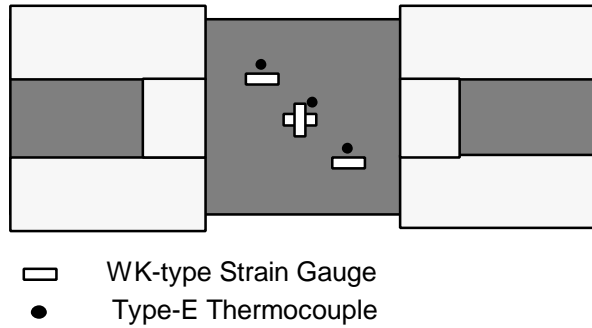


**Figure 11. Test panel instrumentation layout.**

were then drilled through each cell of the core to ensure that the cryogen entered all of the cells during testing.

The test panels were instrumented for the measurement of strain and temperature. Strains were measured using 4 uniaxial WK-06-250BG-350 strain gauges produced by Measurements Group. The gauges were attached to the inner face-sheet of the test panels. Two gauges were located at the center of the panel with one measuring strain in the direction of applied load and the other measuring strain transverse to the applied

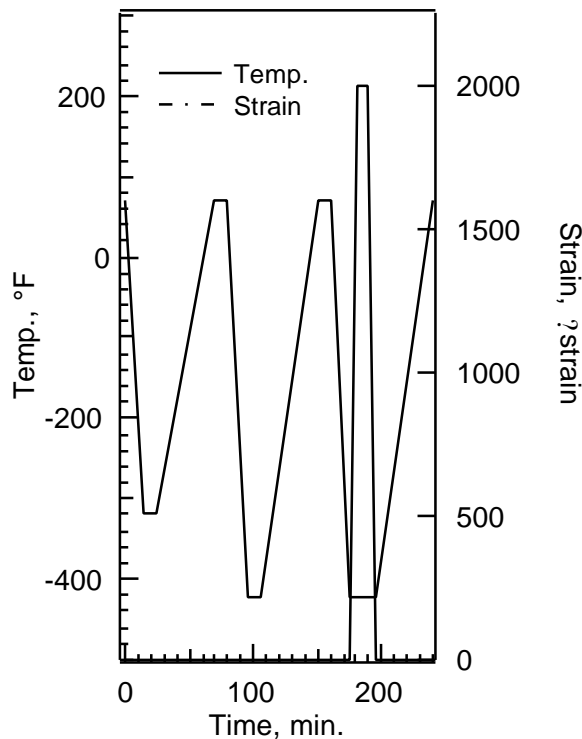


**Figure 12. Thermal and mechanical conditioning profiles for the X-33 panels.**

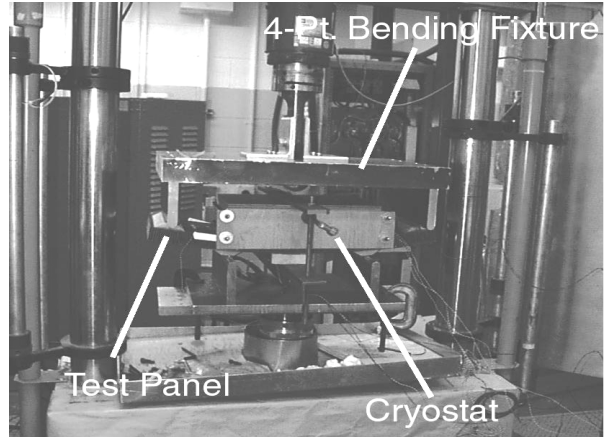


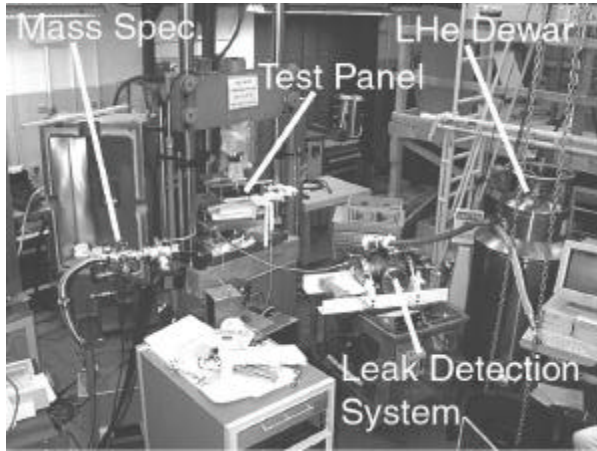
**Figure 13. X-33 panel prior to thermal and thermomechanical conditioning.**

load. Another gauge was located 3 in. above and 3 in. to the left of center, and the fourth gauge was located 3 in. below and 3 in. to the right of center, with each measuring strain in the applied load direction, see Figure 11. Temperatures were measured with Type-E thermocouples that were co-located with the strain gauges.

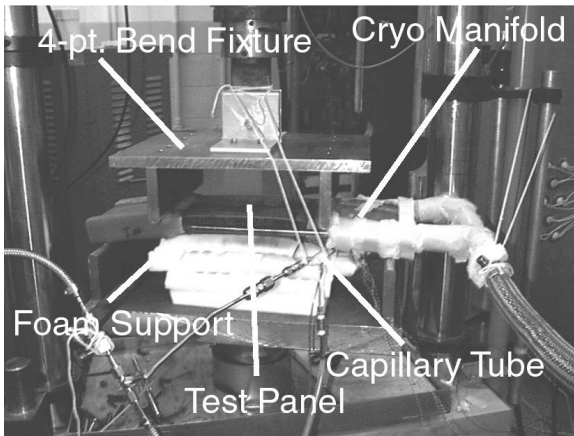
### Thermal and thermomechanical conditioning

The two test articles were subjected to thermal and thermomechanical conditioning to ensure that thermal and mechanical load history of the test articles was as close to the X-33 tank structure as possible. Prior thermal and thermomechanical conditioning enabled the test to produce relevant data for the failure investigation team. The temperatures and mechanical loads applied to the test panel are shown in Figure 12 and a photograph of the one of the test articles, prior to conditioning, is shown in Figure 13. The test panel was placed in the 4-pt. bend fixture and a cryostat (an insulated, five-sided box, with a spray bar to deliver cryogenic fluid to the test specimen) was then placed on top of the specimen. During conditioning, the temperature was maintained by supplying LN<sub>2</sub> or LHe to the cryostat while load was applied through 4-pt. bending.

Both test panels were first thermally cycled to -320°F using LN<sub>2</sub>, then to -423°F (LH<sub>2</sub> temperature) using LHe, then again to -423°F using LHe. On the third thermal cycle, a mechanical load was applied resulting in a tensile strain of 2000 %strain applied to the inner face-sheet of the test panel.



(a) LHe Leak tests at NASA LaRC.



(b) Close-up of specimen in 4-pt. bend fixture.

Figure 14. LHe leak test at NASA LaRC.

#### Liquid helium leak tests

After the test panels were conditioned, LHe leak measurements were made in the Thermal Structures Laboratory at NASA Langley Research Center. Photographs of the tests are shown in Figure 14. The evacuated control volume, the mass spectrometer, the dewar of liquid helium, and the test article mounted in a 100-kip hydraulic load machine are each visible in Figure 14(a). A close-up view of the test specimen located in the load fixture is shown in Figure 14(b), showing a stack of foam that was placed under the specimen to apply a small positive pressure to the FMLDS seal during testing.

Leak measurements were made at inner face-sheet strain values of between zero and 4000- $\mu$ strain and are plotted for each test panel in Figure 15. The leak rate increased with strain until a peak value was reached,  $3.6 \times 10^{-5}$  SCC/sec-in<sup>2</sup> at 2000  $\mu$ strain for panel 1 and  $3.6 \times 10^{-4}$  SCC/sec-in<sup>2</sup> at 3250  $\mu$ strain for panel 2, and

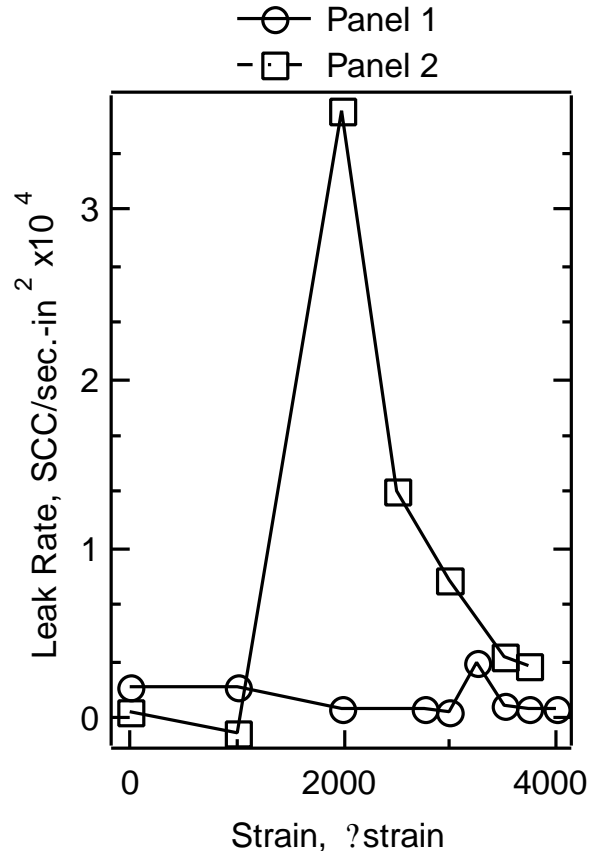
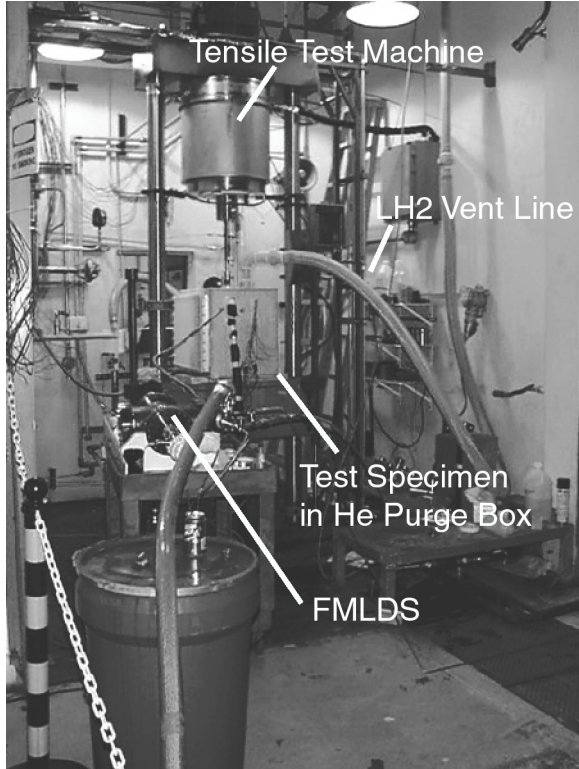


Figure 15. LHe leak data for panel 1 and panel 2.

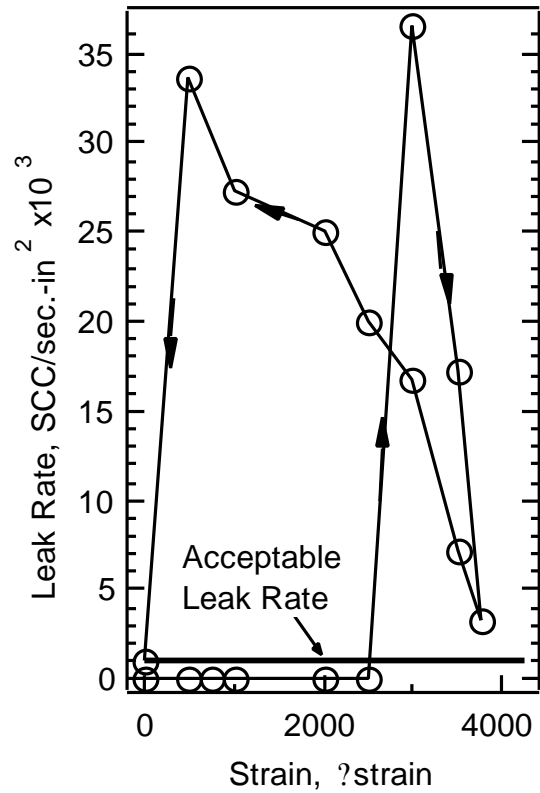
then began to decrease as load was increased to 4000  $\mu$ strain. It was believed that a portion of the microcracks might have closed as the uniaxial load increased due to Poisson's effect, decreasing the leak rate. These values vary greatly (by an order of magnitude at various strains) between the two test panels.

#### Liquid hydrogen leak tests

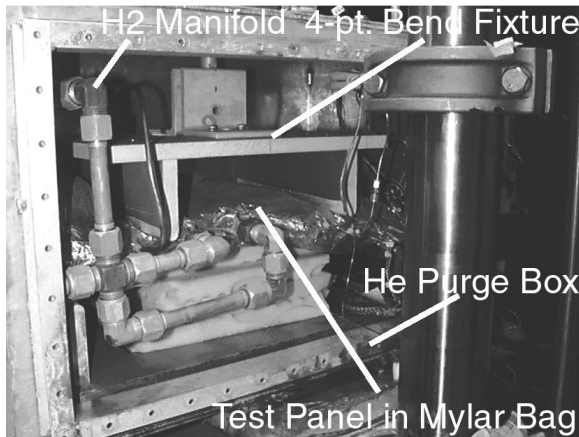
Subsequent to LHe leak tests at NASA Langley Research Center (LaRC), LH<sub>2</sub> leak measurements were made at NASA Marshall Space Flight Center's (MSFC) Cold Flow Hydrogen Test Facility (CFHTF). These tests were performed at MSFC to determine the leak rate using the actual propellant, LH<sub>2</sub>. A photograph of the test setup in a CFHTF test cell, taken at the conclusion of LH<sub>2</sub> leak testing, is shown in Figure 16(a). During LH<sub>2</sub> testing the panel was sealed in a vented aluminized Mylar™ bag which captured the hydrogen and vented it safely to the atmosphere. The test hardware (4-pt. bend fixture, foam support, and test panel) were then contained within an aluminum



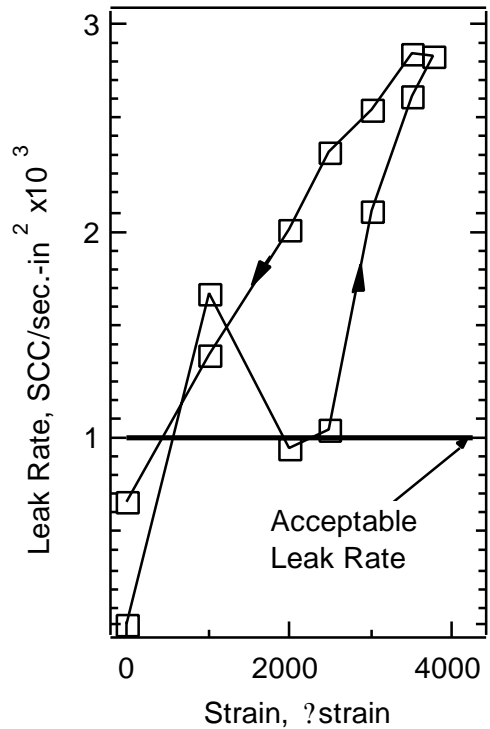
(a) LH<sub>2</sub> leak tests at NASA MSFC



(a) Panel 1 data



(b) Close-up of the specimen in the GHe purge box.  
Figure 16. LH<sub>2</sub> test at MSFC.



(b) Panel 2 data

Figure 17. LH<sub>2</sub> leak data.

chamber which was purged with gaseous helium (GHe) during tests, see Figure 16(b).

Leak measurements were made at strain values between zero and 4000 μstrain. Again, the leak rates varied widely for each panel tested with both panels leaking at increased in the inner face-sheet of panel 1, the leak rate increased, peaking at a rate of  $3.7 \times 10^{-2}$  SCC/sec.-in<sup>2</sup> at 3000 μstrain, and then decreased as load was increased to 4750 μstrain. The load was then removed from the inner face-sheet and the leak rate increased to

a rate of  $3.4 \times 10^{-2}$  SCC/sec.-in<sup>2</sup> at 500  $\mu$ strain before falling to  $1.1 \times 10^{-2}$  SCC/sec.-in<sup>2</sup>, when the load was removed from the panel. This leak rate was substantially higher than the initial leak rate at no load of  $5.3 \times 10^{-5}$  SCC/sec.-in<sup>2</sup>, which indicated that permanent damage had occurred in the inner face-sheet.

The leak rate for panel 2 also increased as inner face-sheet load increased (peaking at a value of  $2.8 \times 10^{-3}$  SCC/sec.-in<sup>2</sup> at 3750  $\mu$ strain) then, as load was removed, the leak rate decreased to  $0.7 \times 10^{-3}$  SCC/sec.-in<sup>2</sup> with no load applied. This rate was higher than the initial leak rate of  $0.17 \times 10^{-3}$  SCC/sec.-in<sup>2</sup> and indicated that permanent damage to the laminate had occurred.

As seen in Figure 17(a) and 17(b), respectively, the leak rates for both panels exceed the acceptable leak rate of  $10^{-3}$  SCC/sec./in<sup>2</sup> given in reference 3. The leak rates for the LH<sub>2</sub> leak tests were an order of magnitude larger than the leak rates for prior LHe tests, which is not explained by gas molecular weight effects between He and H<sub>2</sub>.

### Discussion

Several observations were drawn from the leak measurements that created technical issues. These technical issues dealt with the source of leakage, microstructural behavior of the laminates, and atomic/molecular behavior of GHe versus GH<sub>2</sub>.

The source of leakage for the X-33 panel measurement was either from the composite structure leakage or FMLDS seal leakage. Because of the nature of the measured leakage (leaks returned to nearly zero when load was removed) and based upon prior experience with seal failures in the FMLDS, the data collected were believed to be accurate measurements of panel leakage. Typically, when the FMLDS seal failed, control volume pressures rose instantaneously to very high levels. The pressures measured during LHe and LH<sub>2</sub> testing of X-33 panels never increased at rates similar to those seen when the seal failed. However, during both the calibration tests and each of the X-33 panel tests, a very small leak was observed at the beginning of the tests. This small leak was attributed to a seal leak where the capillary tube penetrated the seal. Therefore, this question has not been conclusively answered.

The measured leak rates indicated a significant leak problem in the X-33 LH<sub>2</sub> tank inner face-sheet. The data gathered for the X-33 tank failure investigation indicated that for the "as-built" structure under thermal and mechanical load, hydrogen leaked at a rate significantly greater than the acceptable leak rate. The apparent leakage mechanism was through microcracks that were generated due to ply level thermal residual

stresses and mechanical stresses generated by the internal pressure load. Leak rates varied with applied load, and test gas used. Also, large variations in leak rates measured for the two panels tested indicated that a wide variation in hydrogen leak rates can be expected (0.0028 to 0.037 SCC/sec.-in<sup>2</sup>).

Measured LHe leak rates do not correlate with LH<sub>2</sub> leak rates. The lack of correlation could be due to either progressive damage in the panels (i.e., increases in as the panel is repeatedly tested microcracking resulting in higher leak levels), or leakage by different mechanisms for LHe and LH<sub>2</sub>. These questions are not answered in this study because these tests had to be completed quickly in support of the X-33 tank investigation. Further research is required to determine if LHe leak testing is effective as a screening test in place of LH<sub>2</sub>.

Additional research is needed to refine the test method and test apparatus and further quantify sources of leak measurement variability. Both improved materials-level and structures-level test systems will provide a better understanding of the complex phenomena of hydrogen leaks in PMCs under thermal-mechanical loading.

### Summary

An apparatus and method of performing micro-leak tests was developed in support of the X-33 Tank Failure Investigation at NASA LaRC. Calibration tests were performed to assess the accuracy of the apparatus across a range of leak rates and at cryogenic conditions. The test method and test apparatus were used to perform leak measurements on a complex, curved, sandwich structure, which was under mechanical load and at cryogenic temperature. Tests of two X-33 LH<sub>2</sub> tank test panels were completed with LHe leak tests performed at LaRC and LH<sub>2</sub> leak tests performed at MSFC.

Calibration tests indicate that the system is accurate, with less than 10 percent error for leak rates from 0.3 SCC/Min. to 200 SCC/Min, with little or no thermal effects if the seal temperature is kept above 0°F. LHe and LH<sub>2</sub> test results indicate that further research is required to determine the acceptability of LHe leak tests as screening tests when LH<sub>2</sub> leaks are the primary concern. Test results also indicate that measured LH<sub>2</sub> leak rates are above acceptable levels for a SSTO LH<sub>2</sub> tank and that they can vary widely with load level and location in the structure.

This investigation has also demonstrated the need for structures-level leak testing to validate composites and composite manufacturing processes for LH<sub>2</sub> tank applications. These tests should include thermal and

thermal-mechanical conditioning and testing of structures under operational mechanical loads and temperatures.

### **References**

1. Cook, Steve *The X-33 Advanced Technology Demonstrator*, AIAA-96-1195, 1996.
2. McCarty, R. D., J. Hord, and H. M. Roder, *Selected Properties of Hydrogen (Engineering Design Data)*, NBS Monograph 168, National Bureau of Standards, Boulder, CO, 1981.
3. Robinson, M. J., *Composite Cryogenic Propellant Tank Development*, Proceedings of the 35<sup>th</sup> AIAA/ASME/ASCE/AHS/ASC Structures, Structural Dynamics and Materials Conference, Hilton Head, SC, 18-21 April 1994.
4. Anon., *Standard Test Method for Determining Gas Permeability Characteristics of Plastic Film and Sheeting*, ASTM-D 1434-82, 1998.
5. Anon., *Final Report of the X-33 Failure Investigation Team*, NASA-MSFC, May 2000, Available at <http://x33.msfc.nasa.gov>, circa January 24, 2001.

### **Acknowledgements**

The authors wish to acknowledge Dr. Steven J. Scotti, from the NASA Langley Research Center, Mr. Michael C. Watwood and Mr. Matthew Jackson, both from the ITT Research Institute for their invaluable contributions to this test program.